Multi-flow optimization of a greenhouse system: A hierarchical control approach

Pierre Clement Blaud, Pierrick Haurant, Philippe Chevrel, Fabien Claveau, Anthony Mouraud

Highlights

Multi-flow Optimization of a Greenhouse System: A Hierarchical Control Approach

Pierre Clement Blaud, Pierrick Haurant, Philippe Chevrel, Fabien Claveau, Anthony Mouraud

- Greenhouses are multi-flow systems combining heat, electricity, gas and CO_2
- Hierarchical control is proposed as an alternative to the usual rule-based controller
- The second level of the controller uses an artificial neural network as dynamic model
- The controller allows efficient dynamic operation and energy and economical savings

Multi-flow Optimization of a Greenhouse System: A Hierarchical Control Approach

Pierre Clement Blaud[a,b,c], Pierrick Haurant[c], Philippe Chevrel[a], Fabien Claveau[a], Anthony Mouraud[b]

[a] *IMT Atlantique, LS2N, UMR CNRS 6004, F-44307 Nantes, France*
[b] *CEA, CEA Tech Pays de la Loire, F-44340 Bouguenais, France*
[c] *IMT Atlantique, GEPEA, UMR CNRS 6144, F-44307 Nantes, France*

Abstract

Greenhouses are implemented all over the world to increase agricultural production thanks to contolled environmental conditions (inside temperature, moisture and CO_2 contents). However, such systems are energy-intensive.

The presented work focuses on controlling a greenhouse' onsite multi-energy system (gas, heat and electricity), extended to a multi-flow system as the CO_2 produced by the energy units is used as a plant fertilizers. In this view, a three levels hierarchical control has been developed: a steady state economic MPC is combined with a dynamic Multi-energy MPC and low-level PID controllers. This new controller aims at determining the best synergies for economic flows management, subject to compliance with the required climatic conditions in the greenhouse.

The proposed controller is applied to a greenhouse which energy system is based on a thermal energy storage fuelled by a gas boiler and a combined heat and power unit. The results are confronted to a usual ruled-based controller performed by greenhouses owners, showing a more efficient dynamic functioning of the energy system. Consequently, less gas is consumed (80.79 t to 76.03 t), heat is produced when needed, and electricity from the CHP is economically optimized allowing less importation from the grid (from 17.80 MWh to 15.88 MWh), and profitable selling.

Keywords: Multi-flow system, Greenhouse, hierarchical control, model predictive control, energy hub, artificial neural network, multi-physics modeling

*Corresponding author

1. Introduction

Agriculture is facing great challenges to feed the world's population in the 21^{th} century, due to its exponential rising, an increase in natural disasters and the stabilization of farmland surfaces [1]. Some technologies such as greenhouses farms are becoming necessary for maximizing agricultural production and reducing resource usage [1]. Indeed, greenhouses aim at making grow the cultures in a regulated environment in which atmosphere gas contents, luminosity and temperature are controlled. As a consequence, the quality and quantity of crop productions can be improved since the plants are less stressed. In addition, harvest times can be increased, water consumption can be reduced and fungicides as well as insecticides are less used due to the protection provided by the greenhouse. However, some additional costs for construction and operation of greenhouses are induced. The challenge is then to control operating costs and carbon dioxide emissions compared to those of traditional crops [2]. Improving the climate of the greenhouse to maximize agricultural production and at the same time minimize energy consumption justifies more than ever the adoption of smart technologies [1].

Control of greenhouse climate systems and actuators has been investigated by many researchers using different control methods and algorithms. In [3], an adaptive proportional–integral–derivative (PID) has been developed to control indoor temperature, moisture, and CO_2 concentration and to minimize tracking errors. In [4], a sliding mode control was employed for its ability to handle non-linearity, coupling, and disturbances to control the greenhouse climate. Fuzzy logic control is also employed in [5]; the control formalizes and approaches the behavior of the person and does not require a pre-established physical model. In [6], a Takagi–Sugeno fuzzy modeling is employed to design a controller for greenhouse temperature control. The controller is tuned according to linear matrix inequalities, which ensures stability and performance in a closed loop and enables control of the greenhouse heating system, which provides good performance. Optimal control is also employed to control the actuators of a greenhouse and has been used in several studies to control the climate of an

agricultural greenhouse. Optimal control is used in [7] to control indoor temperature, moisture, and CO_2 concentration while minimizing energy consumption. In another study, heating and cooling are controlled to reduce energy consumption [8]. The optimal control formalism by Hamilton Jacobi Bellman is also used in [9]. In addition, a multi-objective optimization is investigated to maximize plant production and fruit quality while minimizing water consumption in [10], and in [11] a multi-objective optimization based on Pareto solution is investigated to control both light and temperature conditions. Among advanced control techniques, model predictive control (MPC) is often studied in academia [12] and has been used in several industrial applications [13] and agricultural greenhouse systems [14] [15], [16]; it enables the consideration of constraints on the state variables of the process while modeling the process to control. The use of MPC to control greenhouse climate and actuators is investigated in [17] as it allows for taking into account constraints, non-linear processes and multi-inputs and outputs of the system. Other authors have compared the MPC performance to PID controllers and observed that the former increases temperature control performance [18]. A robust MPC to address uncertainties is also discussed in [19], and the results indicate that the controller regulates the temperature despite the uncertainties with a min-max optimization algorithm.

Hierarchical control is also considered to control greenhouse climate. In [10], a three-level control is depicted. The first level controls the fertilizers and the climate of the greenhouse on a time scale of one minute. The second level adjusts the setpoints on the time scale of the day. The third level, on the time scale of the month, controls the growth of the plant. In another work [e.g., [20]], a two-levels hierarchical control has been investigated. The upper level computes the setpoints by minimizing the economic cost of energy, while the lower level receives the setpoints and controls actuators with PID and bang-bang controllers. Besides, some works consider neural networks based solutions to control climate variables such as indoor temperature, moisture, CO_2 [21],[22], [23], or even of the leaf and fruits growth as in [24].To the authors' knowledge, no paper take benefits from an ad hoc neural network to fully control the greenhouse indoor environment. They proceed by more targeted objectives as in [25] which uses a neural network based MPC for ventilation control.

The control of energy systems supporting agricultural greenhouses has been explored in few studies [26, 27, 28, 29, 30] compared to climate control [3, 4, 5, 6, 7, 8, 9, 10, 17, 18, 19, 20]. In [26], wind turbines, photovoltaic panels, battery storage, grid connection, and combined heat and power (CHP) are considered as part of the agricultural greenhouse. The control is based on MPC to effectively control energy and improve availability, flexibility, and efficiency. The same authors extended their work in [27] by considering a network of several greenhouses interconnected in a microgrid. The modeling of the greenhouseThe study presented here follows our review of the literature. It focuses specifically on the optimized management of the (multi)energy system of the greenhouse to meet the energy needs of the greenhouse. Therefore, the main ambitions and contributions of this work are: load is conducted by a nodal resistance-capacity model, and the growth process of the plant is not taken into account. In [28], the authors improved the greenhouse modeling, considering temperature, moisture, CO_2, air circulation, artificial lighting, and energy support systems comprising wind turbines, photovoltaic panels, energy storage with battery units, and pumping and water storage systems. A centralized MPC scheme is depicted to control the greenhouse energy system and greenhouse environmental variables. However, wind turbines and photovoltaic panels considered in these papers ([26, 27, 28]) as energy providers do not reflect current equipments available in high-tech greenhouse systems. The latter make use of heating systems such as a heat-pump [31], boiler, CHP, and thermal storages [29]. One can speculate that agricultural areas are retained for crops instead of energy production via solar panels or wind turbines as the former is more profitable for the farmer. In [29] the study aims to minimize the energy (natural gas and electricity) cost while taking into account the system constraints. Results obtained illustrate an increase in profit as compared to conventional control. The study is extended in [30] by adding a heat pump, seasonal thermal storage, and cooling towers. The results show a cost reduction of 29 % over a year.

As it can be seen in the literature review, control of greenhouses is addressed in numerous studies, either to regulate their indoor environment (temperature, moisture and CO_2 contents, etc.) or to optimize their own energy systems from economical or energy points of view. Usually, linear and non linear predictive control are implemented. This

is a logical choice regarding the nature of the problem considering time characteristics, the fact that exogenous phenomena that can be partly predicted are involved, and the need to constraint states or control signals.

The study presented here follows our review of the literature. It focuses specifically on the optimized management of the (multi)energy system to meet the energy needs of the greenhouse. Therefore, the main ambitions and contributions of this work are:

- To consider a realistic greenhouse equipped with a complete energy system, based on a combined heat and power unit, a gas boiler and a thermal energy storage (TES). In that view, we have to do with a real multi-energy system: the energy sources are electricity, and natural gas, and we also have to manage internally both high and low temperatures heating networks. The system can even be seen as being a multi-flow system, since we also seek to control the flow rate of CO_2, in interaction with the energy system via the boiler.

- To propose a three levels hierarchical control architecture : a static optimization of the power flow at the third level thanks to an Economic MPC, a dynamic optimization of the Multi-Energy system at the second layer using a MPC (ME-MPC), to finally adress a classical low-level layer for the climate regulation of the greenhouse, based on rule-based or proportional-integral-derivative controllers. This hierarchical control law is innovative to the extent that the dynamic optimization with MPC of the second level is based on a dynamic model implemented thanks to an artificial neural network (ANN).

- To develop a systematic method for the second-level MPC control, which performs a data-based simplification of the fine model of the multi-energy system. The proposed model based on an artificial neural network (ANN) and a limited number of state variables is an important contribution, in that it takes into account the multi-physics dynamics (CHP, boiler, etc.) of the energy system, for a reduced computational cost.

- And finally to propose a realistic validation of the global hierarchical control, by comparing its performances with those of a rule-based control, inspired by real

practice.

To adress these issues, the article is organized as follows: section 2 presents the considered greenhouse energy system and its base-line controller. Section 3 details the proposed controller of the research work. Section 4 depicts multiphysics simulator, while the case study and associated results are introduced and discussed respectively in section 5 and 6. Finally, section 7 provides the conclusions of the work.

2. The studied energy system

2.1. Energy and ancillaries systems functionning

Temperature and the luminosity that fosters the photosynthesis of plants, as well as the moisture and the CO_2 contents of the atmosphere are the main ambient elements to be controlled in the greenhouse for the development of cultures. Energy systems and ancillaries are implemented in that view. Thus, the greenhouse is heated thanks to solar gains on one hand, and high and low temperatures heating networks on another hand. The high temperature heating network is fueled by thermal energy storage (TES) itself charged by heat from a gas combined heat and power unit (CHP) and a gas boiler. The low temperature one valorized the heat of the exhaust fumes produced by the two energy units mentioned above. In case of overheating during the day, a solar screen allows limiting the solar gains and windows can be opened in order to force the air circulation in the greenhouse, inducing natural ventilation. These windows can be opened in case of too high moisture level, produced by the plants by evapo-transpiration. Besides, a thermal screen can be deployed when outside temperature is very low, in order to limit the thermal losses from the greenhouse. The luminosity is guaranteed by the solar irradiance substituted or completed by artificial light when necessary. The lights consume electricity produced by the CHP or supplied by the grid. Thus, the electricity from the CHP is either consumed by ancillaries of the greenhouses, or sold and injected to the grid. Finally, the atmosphere in the greenhouse is enriched with CO_2 used as a fertilizer, through injectors to valorize CO_2 emitted by the energy units fed by gas, or through a CO_2 network.

The greenhouse's energy system can be considered as a multi-energy system with gas, electricity and heat as carriers; the CHP and a gas boiler consume gas to produce locally heat and electricity. The greenhouse consumes heat and electricity produced locally or electricity from the grid. Also, the excess electricity can be sold to the grid. If we add the CO_2 flows, a matter flow, to the energy ones, we can consider the greenhouse as a multi-flow system.

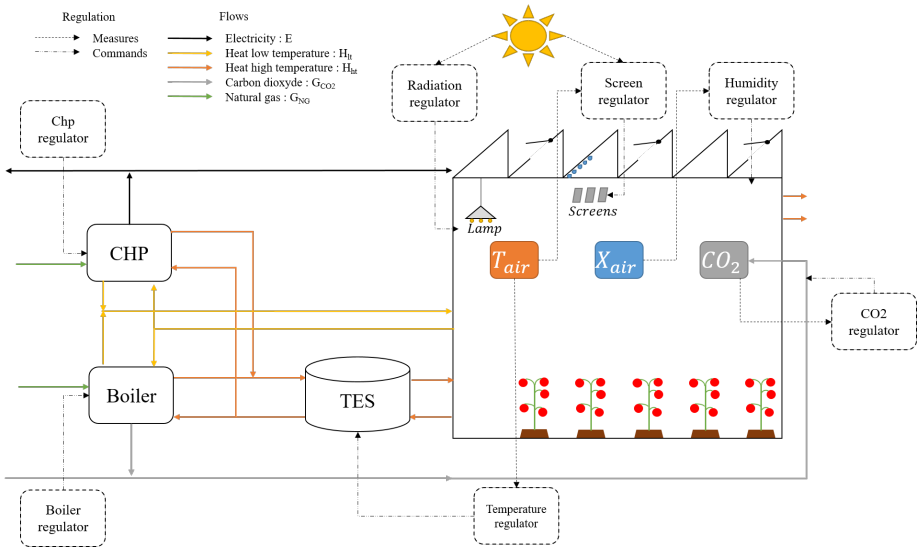

Figure 1: Greenhouse considered in this study.

2.2. Base-line controller

The current controller of the multi-flow system is a rule-based one that mimics the farmer practices. The rules are not based on elaborate algorithms, but on choices of farmers derived from their experience. In fact, they control their energy system to optimize the energy production with reduced operating costs (electricity, natural gas, CO_2), and valorizing purchase contracts on the electricity selling. The rules can be summarized as follow (Fig.2):

- The CHP is controlled according to the months of the year, with full load operation from the beginning of November to the end of March. After that, the power

is zero for the rest of the year;

- The Boiler is regulated according to the CO_2 demand of the greenhouse and the SOC of the TES. When there is a demand for CO_2, the boiler starts at low power and stops if the heat storage is full. Conversely, if the thermal storage reaches a low threshold, the boiler starts at full power.

- TES: Protection is needed in the management of the thermal storage unit. Heat is rejected in the agricultural greenhouse when the storage is full and the cogeneration produces heat. It can happen that the agricultural greenhouse is over-heated. If the temperature in the agricultural greenhouse is too high (2 °C above the set-point), then the windows of the greenhouse are open to evacuate the excess heat into the atmosphere.

- The Ancillary systems (Radiation, temperature, screens, humidity and CO_2) are controlled by PID or rule-based regulators. Thus, the greenhouse temperature is regulated by a PID that controls the flow of a pump to heat the greenhouse when required. The humidity is controlled by a PID that activates the opening of the windows when the humidity level is too high. The CO_2 concentration is controlled by a PID which operates CO_2 injectors. A rule-based regulator controls the artificial radiation in the greenhouse with several lamps. The Tomatoes' thermal comfort is guaranteed by a rule-based control applied to the thermal screen and sun screen. Finally, to protect the tomatoes, windows are open when excessive temperatures occur.

Our objective is to propose a control architecture and an associated tuning methodology that could handle most greenhouses' energy and CO_2 systems. Its complexity is rich enough to be both representative and challenging for the control methodology proposed.

3. Multi-energy model predictive control hierarchical control

The proposed control strategy is based on a three-level hierarchical architecture, taking advantage of what we call multi-energy model predictive control (ME-MPC).

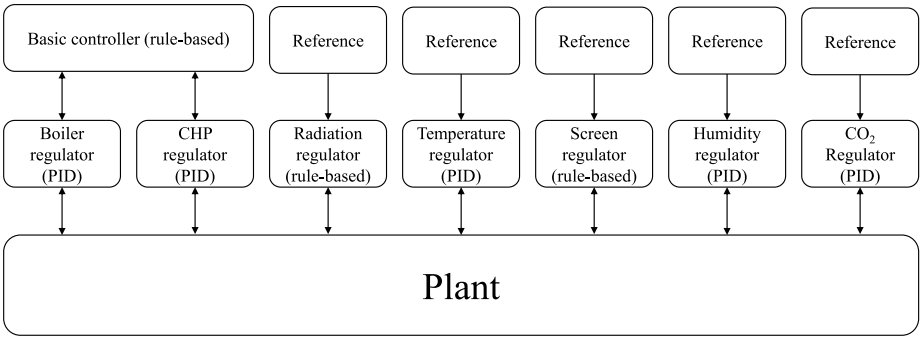

Figure 2: Controller with low-level controller.

Such a hierarchical structure has the benefit of facilitating the design of commands. It makes it possible to dissociate the stages of planning and regulation, the automated regulation part itself being hierarchized according to significantly different time scales [32]. The first level comprises the low-level regulator; it introduces feedback control or rule-based control and is responsible for operating the actuators of the process regarding references received from the upper level. The second level enables dynamic optimization with process modeling, multiple inputs/outputs and constraints regarding references received from the upper level, and predictions (e.g., from the weather forecast). The third level enables steady-state optimization regarding an economic cost function; it computes the optimal setpoints, which are sent to the lower level. A summary illustration of the controllers depicted in this work, with the three levels, is shown in Fig.3. Subsequently, each control level from top to bottom is described.

3.1. Third level: steady-state optimization via Economic-MPC

The third level performs a steady state optimization with the purpose of minimizing economic costs while taking the constraints into account. Constraints include process modeling with algebraic equations and operating constraints. The multi-energy process modeling is easily performed thanks to the energy hub framework and the power balance equations [33]. An illustration of the energy hub considered in this work is shown in Fig.4, and the equations are detailed below.

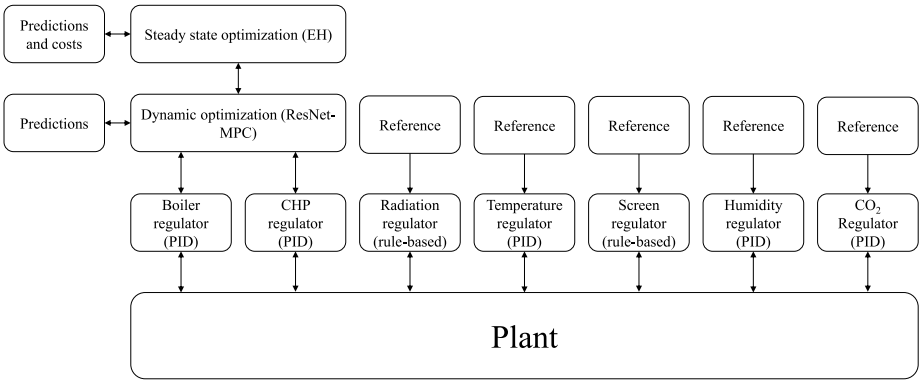

Figure 3: Proposed controller of the greenhouse and multi-energy process, with low-level, second and third level regulators.

Power balance constraints:. The output vector L and the power balance associated with the energy hub are:

$$\underbrace{\begin{bmatrix} E_{gh} \\ H_{gh} \\ 0 \\ G_{CO_2,gh} \end{bmatrix}}_{L} = \underbrace{\begin{bmatrix} 0 \\ H_{boiler} \\ 0 \\ G_{CO_2,boiler} \end{bmatrix}}_{P_{boiler}} + \underbrace{\begin{bmatrix} E_{chp} \\ H_{chp} \\ 0 \\ 0 \end{bmatrix}}_{P_{chp}} + \underbrace{\begin{bmatrix} E_{grid} \\ 0 \\ G_{ng,grid} \\ G_{CO_2,grid} \end{bmatrix}}_{P_{grid}} + \underbrace{\begin{bmatrix} E_{ex} \\ 0 \\ 0 \\ G_{CO_2,ex} \end{bmatrix}}_{P_{ex}} + \underbrace{\begin{bmatrix} 0 \\ H_{ch} \\ 0 \\ 0 \end{bmatrix}}_{P_{ch}} + \underbrace{\begin{bmatrix} 0 \\ H_{dis} \\ 0 \\ 0 \end{bmatrix}}_{P_{dis}} \tag{1}$$

E_{gh}, H_{gh}, and $G_{CO_2,gh}$ are the electricity power, heat, and CO_2 flow consumed by the greenhouse. H_{boiler} and $G_{CO_2,boiler}$ define heat and CO_2 flow from the boiler. E_{chp} and H_{chp} represent the electric power and heat produced by the CHP. E_{grid}, $G_{ng,grid}$, and $G_{CO_2,grid}$ reflect the electric power, natural gas and CO_2 flow from the electrical, gas and CO_2 networks. E_{ex} is the electric power injected into the grid, and $G_{CO_2,ex}$ is the CO_2 produced by the boiler that is not reused and is sent into the air. H_{ch} and H_{dis} are, respectively, the charging and discharging heat from the TES.

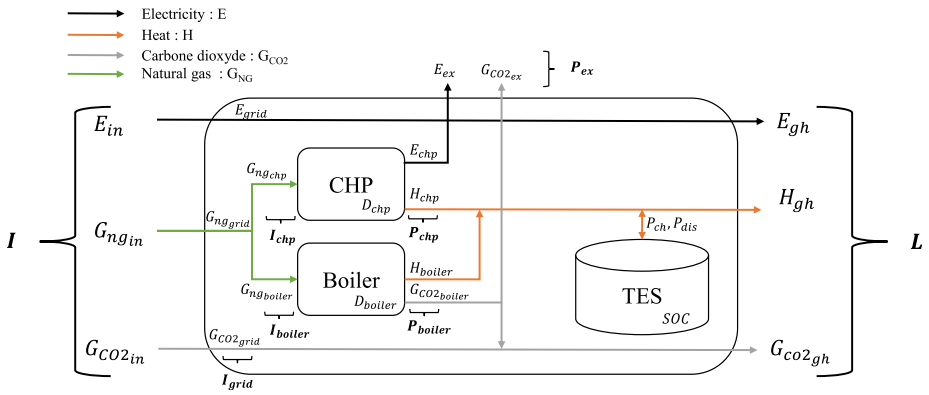

Figure 4: Energy hub modeling associated to the studied multi-energy system.

P_{boiler}, P_{chp} and P_{grid} are given by:

$$P_{boiler} = \underbrace{\begin{bmatrix} 0 & 0 & 0 & 0 \\ 0 & 0 & C_{boiler_{G\_to\_H}} & 0 \\ 0 & 0 & 0 & 0 \\ 0 & 0 & C_{boiler_{G\_to\_CO2}} & 0 \end{bmatrix}}_{D_{boiler}} \underbrace{\begin{bmatrix} 0 \\ 0 \\ G_{ng,boiler} \\ 0 \end{bmatrix}}_{I_{boiler}} \tag{2}$$

$$P_{chp} = \underbrace{\begin{bmatrix} 0 & 0 & C_{chp_{G\_to\_E}} & 0 \\ 0 & 0 & C_{chp_{G\_to\_H}} & 0 \\ 0 & 0 & 0 & 0 \\ 0 & 0 & 0 & 0 \end{bmatrix}}_{D_{chp}} \underbrace{\begin{bmatrix} 0 \\ 0 \\ G_{ng,chp} \\ 0 \end{bmatrix}}_{I_{chp}} \tag{3}$$

$$P_{grid} = \underbrace{\begin{bmatrix} C_{grid_{to\_E}} & 0 & 0 & 0 \\ 0 & 0 & 0 & 0 \\ 0 & 0 & 0 & 0 \\ 0 & 0 & 0 & C_{grid_{to\_CO_2}} \end{bmatrix}}_{D_{grid}} \underbrace{\begin{bmatrix} E_{grid} \\ 0 \\ G_{ng_{grid}} \\ G_{CO2_{grid}} \end{bmatrix}}_{I_{grid}} \tag{4}$$

where D_{boiler}, D_{chp}, and D_{grid} are the conversion matrices related, respectively, to the boiler, the CHP, and the grid. $C_{boiler_{G\_to\_H}}$ represents the natural gas to heat conversion

from the boiler, $C_{boiler_{G\_to\_CO2}}$ the natural gas to CO_2 conversion from the boiler, $C_{chp_{G\_to\_E}}$ the natural gas to electricity conversion from the CHP, $C_{chp_{G\_to\_H}}$ the natural gas to heat conversion from the CHP, $C_{grid_{to\_E}}$ the electricity grid to electricity carrier conversion inside the energy hub, and $C_{grid_{to\_CO2}}$ the CO_2 grid to CO_2 flow conversion inside the energy hub. I_{boiler}, I_{chp}, and I_{grid} define the input vectors of the grid, the boiler, and the CHP. Furthermore, the input vectors (I) of the energy hub associated with the grids, boiler, and CHP are:

$$I = I_{grid} + I_{boiler} + I_{chp} \tag{5}$$

The recurrent equation associated with thermal storage is:

$$SOC_{tes}[k+1] = SOC_{tes}[k] + \Delta_k H_{ch}[k] - \Delta_k H_{dis}[k] \tag{6}$$

where SOC_{tes} depicts the state of charge (SOC) of the thermal energy storage in MWh, k the discrete sampling time and Δ_k the sample time in $hours$.

Operational constraints:. Operational constraints are associated with the equipment (boiler, CHP, or storage element). They are extracted from the specificities of the energy devices, and they are filled in for the optimizer. Equipment powers are semi-continuous optimization variables that can take a value between a minimum and a maximum or zero. To program these variables into the optimization problem, integer variables are used, such as:

$$P^{min}_{boiler} State_{boiler} \leq P_{boiler} \leq P^{max}_{boiler} State_{boiler} \tag{7}$$

$$P^{min}_{chp} State_{chp} \leq P_{chp} \leq P^{max}_{chp} State_{chp} \tag{8}$$

where $P^{min}_{\bullet}$ and $P^{max}_{\bullet}$ are respectively the minimal and maximal powers of the boiler or the CHP. $State_{\bullet}$ is a binary variable of the operating state (0 or 1) of the energy systems.

The minimal operating time (minimum time between two shutdowns) is provided by the following equation:

$$\sum_{i=k-minUp_{boiler}+1}^{k} on_{boiler}[i] \leq State_{boiler}[k] \tag{9}$$

$$\sum_{i=k-minUp_{chp}+1}^{k} on_{chp}[i] \leq State_{chp}[k] \tag{10}$$

where $minUp_{\bullet}$ reflects the minimal operating time parameter (as a multiple of sampling time), $on_{\bullet}$ is a continuous variable allowing the detection of the starting instants of the given equipment.

The minimal shutdown time (minimum time between two shut-ups) is provided by the following equation:

$$\sum_{i=k-minDown_{boiler}+1}^{k} off_{boiler}[i] \leq 1 - State_{boiler}[k] \tag{11}$$

$$\sum_{i=k-minDown_{chp}+1}^{k} off_{chp}[i] \leq 1 - State_{chp}[k] \tag{12}$$

where $minDown_{\bullet}$ is the minimal shutdown time parameter (as a multiple of sampling time), $off_{\bullet}$ is a continuous variable allowing the detection of the shut down instants of the given equipment.

The TES constraints related to energy stored is defined as such:

$$SOC_{tes}^{min} - Slack \leq SOC_{tes} \leq SOC_{tes}^{max} + Surplus \tag{13}$$

with SOC_{tes}^{min} and SOC_{tes}^{max} are respectively the minimal and maximal state of charge of the TES. $Slack$ and $Surplus$ are the constraint relaxation variables: they allow a small violation of the constraints.

Furthermore, terminal constraints are added to the final state of charge to avoid to discharge all the storage energy in its computing horizon, such as:

$$SOC_{tes}^{min,ter} - Slack[N_{eh}] \leq SOC_{tes}[N_{eh}] \leq SOC_{tes}^{ter} + Surplus[N_{eh}] \tag{14}$$

with $SOC_{tes}^{min,ter}$ and $SOC_{tes}^{max,ter}$ terminal constraints parameters with minimum and maximum values and N_{eh} the horizon length of the steady-state optimization.

Additional constraints are necessary when programming the optimization problem. These constraints are not related to the physical limits of the equipment but contribute to the solution.

Firstly, all the decision variables ($Slack$, $Surplus$, P_{boiler}, P_{chp}, P_{grid}, P_{ch}, P_{dis}, P_{ex}, I, I_{chp}, I_{boiler} and I_{grid}) are constrained to be greater or equal to zeros. Then, a constraint is added on the on and off variables to force them to take 0 or 1 values as binary variables:

$$State_{boiler}[k] - State_{boiler}[k-1] = On_{boiler}[k] - Off_{boiler}[k] \tag{15}$$

$$State_{chp}[k] - State_{chp}[k-1] = On_{chp}[k] - Off_{chp}[k] \tag{16}$$

Cost function:. The cost functions considered in this study are the startup cost (specifies the startup expense) and the production cost (specifies the operating expense). Then the revenues are derived from the sale of electricity on the grid. The startup cost related to the equipment startup is detected with the on optimization variable, such as:

$$Cost_1 = on_{boiler}\ start^{cost}_{boiler} + on_{chp}\ start^{cost}_{chp} \tag{17}$$

where $Cost_1$ is the start up cost of the boiler and the CHP, on_j is a continuous variable allowing the detection of the starting instants of the equipment, and $start^{cost}_j$ the starting expenditure parameter of energy equipment related to the boiler or the CHP. The production cost is linked to the purchase price for each energy carrier as well as the gain from the energy sale, as follow:

$$Cost_2 = \begin{bmatrix} elec_{cost} \\ gas_{cost} \\ CO_{2_{cost}} \end{bmatrix} I \tag{18}$$

where $Cost_2$ is the operating expense, $elec_{cost}$ the electricity rate, gas_{cost} the natural gas rate, $CO_{2_{cost}}$ the CO_2 rate, and I the input vector of the EH. The revenue process comprises the sale of electricity, shown as:

$$Cost_3 = \begin{bmatrix} -elec_{cost} \\ 0 \\ 0 \end{bmatrix} P_{ex} \tag{19}$$

with $Cost_3$ the sales gain of the EH, $elec_{cost}$ the electricity rate and P_{ex} the exhaust vector.

It is preferable to keep a convex cost function to maintain the linear optimization problem with integers (mixed integer linear programming , MILP). The cost function include: $Cost_1$, $Cost_2$, $Cost_3$, and the $Slack$ and $Surplus$ are added for the soft constraint relaxation variables; the horizon length is also taken into account. The cost function is defined as:

$$\mathcal{J} = \sum_{k=0}^{N_{eh}-1} Cost_1[k] + Cost_2[k] + Cost_3[k] + \rho \sum_{k=0}^{N_{eh}} Slack[k] + Surplus[k] \tag{20}$$

with $Cost_{1_k}$ from Eq. (18), $Cost_2$ from Eq. (19), $Cost_{3_k}$ from Eq. (17), ρ the cost related to the $Slack$ and $Surplus$ variables.

Optimization problem:. The whole optimization problem based on MILP is to minimize the cost function $\mathcal{J}$ with the hitherto presented constraints. It is defined as:

$$\min \mathcal{J} \tag{21}$$

$$\text{subject to } (1), (2) - (4), (5) - (16) \tag{22}$$

$$L[0] = \bar{L}(t) \tag{23}$$

$$SOC_{tes}[0] = S\bar{O}C_{tes}(t) \tag{24}$$

with Eq.(23) the greenhouse loads initialization with the measure $\bar{L}(t)$ and prediction and Eq.(24) the SOC initialization with the measure $S\bar{OC}_{tes}(t)$.

3.2. Second level: dynamic optimization via Multi Energy-MPC

The dynamic optimization level is performed via MPC. Compared to the previous level, the control actions are computed here taking into account the dynamic behavior of the energy systems, thanks to an embedded model that makes some predictions possible on a receding time horizon. In this work, we consider that the state is known in real time, and the state predictor is defined by a recurrent equation of the form:

$$\hat{x}[k+1] = g_{nn}(\bar{x}[k], \bar{u}[k], \bar{v}[k]) \tag{25}$$

One challenge is to find a suitable g_{nn}; it could be a linear physical model with state space representation [34], a non-linear one [35] or a grey-box model identified from data [36].~~One challenge is to find a suitable g_{nn}; it could be a linear physical model with state space representation [34] or a non-linear one [35].~~[PB] The method explored in this work uses a black-box model following a methodology extracted from [37].

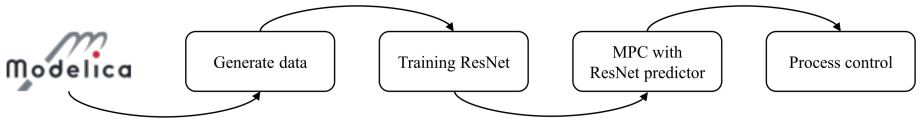

Figure 5: Main steps of the MPC tuning.

The main steps are summarized in Fig.5. First, data are generated from the fine-scale modeling of the dynamical system to be controlled. In this work, the greenhouse system is modeled with a multi-physics implementation with Modelica programming language [38]. The language enables performing fine-scale multi-physics modeling such as electricity, thermal, or gas. In addition, a Modelica library implements the greenhouse system balance equations and other equipment[2] that forms the system [39]. The equipment and materials encountered are tomato crops, canopies, soil, heating networks, air nodes, CO_2 nodes, lights, thermal screen, sun screen, covers, and windows opening. In addition, the physical flux between each piece of material is modeled. The greenhouse proposed in [39] has been enhanced for this study. We added a separate heating pipe with a low-level and high-level temperature. The Multi-Energy System is modeled with a fine-scale multi-physics approach using the TransiEnt library [40]. The library proposes the thermal storage with thermal stratification, the boiler, and the CHP. The boiler and the CHP are enhanced to take into account two heating networks with low and high temperatures.

Secondly, a neural network is trained to learn the recurrent equation (Eq.25). It represents only the MES part to be controlled, and not the whole greenhouse. Thirdly, the MPC is tuned with the neural state predictor. We chose in this paper to learn the model instead of the optimal policy, that is to say to use neural networks coupled with

predictive control instead of other machine learning approaches such as deep reinforcement learning to handle the computational burden. This choice is motivated by results provided in [41] or [42], where pros and cons of both strategies for the control of industrial processes are analyzed. Finally, the neural network used in this work is residual network (ResNet) [43]. The ResNet network has been assessed to improve the generalizability of the network compared to more conventional neural networks [44, 45]. In this work, the state, input, and non-controllable inputs from Eq.(25) are defined as:

$$\bar{x} := \begin{bmatrix} SOC_{tes} \\ H_{boiler} \\ H_{chp} \\ E_{chp} \\ G_{CO_{2_{boiler}}} \end{bmatrix}, \ \bar{u} := \begin{bmatrix} u_{boiler} \\ u_{chp} \end{bmatrix}, \ \bar{v} := \begin{bmatrix} H_{gh} \\ E_{gh} \\ G_{CO_{2_{gh}}} \end{bmatrix} \tag{26}$$

The MPC selected in this work is contractive to ensure the stability and feasibility of the predictive control [46] due to contractive state constraints. The MPC formulation is:

$$\min_{\tilde{u},\tilde{x}} \sum_{i=0}^{N-1} \tilde{x}_i^T Q \tilde{x}_i + \tilde{u}_i^T R \tilde{u}_i \tag{27}$$

$$\text{s.c. } \hat{x}_{i+1} = g_{nn}^*(\hat{x}_i, u_i, \bar{v}_i) \tag{28}$$

$$\hat{x}_i \in \mathcal{X} \tag{29}$$

$$u_i \in \mathcal{U} \tag{30}$$

$$\hat{x}_0 = \bar{x}(t) \tag{31}$$

$$\tilde{x}_N P \tilde{x}_N \leq \alpha \tilde{x}_0 P \tilde{x}_0 \tag{32}$$

$$\tilde{x}_i = \hat{x}_i - x_i^r \tag{33}$$

$$\tilde{u}_i = u_i - u_i^r \tag{34}$$

with Eq. (27) the quadratic cost to minimize. $\tilde{u}$ is the input deviation sequence from the optimal steady state u^r, Eq. (34), such as $\tilde{u} := \tilde{u}_0, \ldots, \tilde{u}_{N-1}$. $\tilde{x}$ is the state deviation sequence from the optimal steady state x^r, Eq. (33), such as $\tilde{x} := \tilde{x}_0, \ldots, \tilde{x}_N$ with N the horizon length. Eq. (28) is the time evolution constraint of the state, which is based on the artificial neural network. Eq. (29) is the state constraints and Eq. (30) is the input

constraints. Eq. (31) is the plant state measure. Eq. (32) is the contractive constraint with α the contractive parameter, $\alpha \in [0, 1[$ and P the contractive weighting matrix. The contractive MPC is computed at each iteration, and the first sample of the input computed (u^*) is applied to the low-level references until the next sampling period.

3.3. First level: low-level control

The low-level control comprises several PID controller [47], and rule-based ones that control specifically the ancillary systems. The controllers that are exposed in section 2.2 are kept.

4. Multiphysics simulator

The fine-scale Modelica model that has been used to tune the neural network embedded in the second-level controller is also used as a validation model in this paper. It was exported using a functional mock-up unit (FMU) for simulation and performed using Simulink. The third and second levels of the proposed controllers interact with the FMU, and then the low-level controllers are implemented within the fine-scale modeling in Modelica programming (Fig.6). In addition, a co-simulation was chosen within the FMU, and the solver CVODE is used [48]. At each sample time, the FMU simulation is paused and then the hierarchical control computed; the new input commands are sent to the low-level regulator, and the simulation continues until the next pause (Fig.7). During the simulation, the data was saved to depict results.

4.1. Computing implementation

The hierarchical control levels are computed at a fixed time, and the third and second levels are computed in a receding horizon manner at different time scales. In addition, the third level sends references to the second level, and the second level sends reference to the first level when it governs the actuators (Fig.7).

4.2. Implementation of the third level: steady-state optimization

The third level is implemented using modeling language specific to the field of optimization, namely JuMP [49] on Julia programming [50]. Constraints on the CHP and

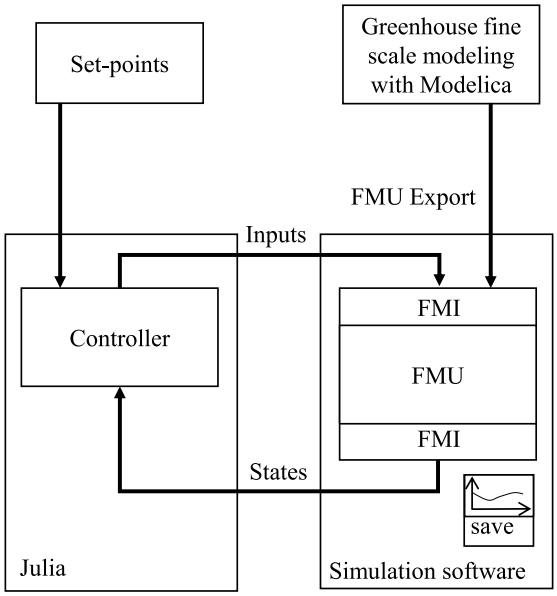

Figure 6: Simulator, FMU and controller on Julia.

the boiler generate integer variables; as a result, the optimization problem becomes an MILP. Several solvers are available such as Coin-or branch and cut (CBC) with the linear solver Coin-or linear programming (CLP) [51] or CPLEX from IBM. In this work, we use the latter one as it allows for a result equivalent to CBC while reducing the computation time. This reduction is obtained by automatic simplification methods of the optimization problem: reduction of the number of integer variables, normalization, heuristics of reduction of the optimization problem with the branch and cut algorithm, and a computation on several CPU cores. The time horizon is equal to 96 sampling steps of 15 minutes, i.e. 24 hours or a day, hence an optimized compution time of approximately 5 seconds. The steady-state optimization algorithm is depicted in Algorithm 1.

4.3. Implementation of the second level: dynamic optimization

The neural network is implemented on computing machines using Flux [52], a package of the Julia programming language [50] that provides highly competitive lan-

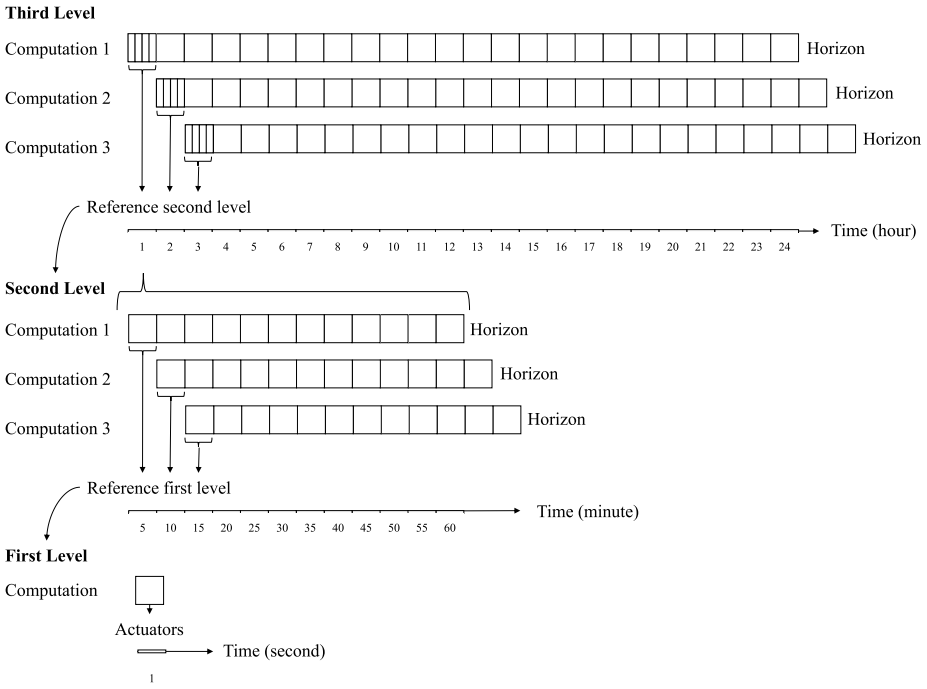

Figure 7: Hierarchical control, reference transmission and horizon length of the three levels.

Algorithm 1 Steady-state optimization computation

1: Initialize the optimization problem with SOC Measure $SOC[0] \Leftarrow S\bar{O}C(t)$ and load measure and prediction $L[k] \Leftarrow \bar{L}(t)$
2: Solve the MILP optimization problem
3: Send the optimization results computed to second level, SOC^*_{tes}, H^*_{boiler}, H^*_{chp}, E^*_{chp} and $G^*_{CO_{2_{boiler}}}$
4: Wait until the next iteration $t \Leftarrow t + 1$
5: Go to step one

guage for data science and scientific computing [53]. The package allows the implementation of the neural networks, training, and identification of performance measures.

The MPC is implemented on a modeling language specific to the field of optimization, namely JuMP [49] on the Julia programming language [50]. The MPC predictor

is defined with the JuMP user-defined function from the Flux object function. In this case, it allows us to compute the gradient with automatic differentiation [54], and it is not required to rewrite the neural network since Flux and JuMP are both in Julia's ecosystem. The optimization problem is non-linear due to the activation function, and the selected solver is Knitro [55]. The MPC is solved at each 300 s and the allowed optimization time is equal to 30 s. After 30 s of computation, if the solver does not stop the optimization, the sub-optimal computed value is selected. The horizon length and weighting matrices selected in this work are shown in Table 1. The MPC algorithm is depicted in Algorithm 2.

Algorithm 2 MPC computation

1: Measure the system states $\hat{x}_0 \Leftarrow \bar{x}(t)$
2: Get the predictions of the non-controllable inputs $\bar{v}$
3: Solve the optimization problem (MPC)
4: Send the first input command computed u_0^* to the low-level control
5: Wait until the next iteration $t \Leftarrow t + 1$
6: Go to step one

4.4. Implementation of the first level: low-level control

The low-level controllers are implemented within the Modelica program, according to the controllers and rules expressed in section 2.2.

5. Case study

The greenhouse considered in this study was inspired by those found in Nantes, Pays de la Loire region, France. Table 2 describes the main characteristics of its energy system. To remain standard, certain less commonly used energy equipment (geothermal heat pump, recovery of CO_2 from cogeneration, photovoltaic or thermal solar panels, etc.) is not taken into account. The proposed methodology is not, however, limited to this standard case.

Table 1: MPC parameters used during simulation.

Parameters	Values
N	12
ΔT	$300s$
Q	$\begin{bmatrix} 5 & 0 & 0 & 0 & 0 \\ 0 & 1 & 0 & 0 & 0 \\ 0 & 0 & 2 & 0 & 0 \\ 0 & 0 & 0 & 2 & 0 \\ 0 & 0 & 0 & 0 & 1 \end{bmatrix}$
R	$\begin{bmatrix} 0.5 & 0 \\ 0 & 0.5 \end{bmatrix}$
P	$\begin{bmatrix} 1 & 0 & 0 & 0 & 0 \\ 0 & 0.001 & 0 & 0 & 0 \\ 0 & 0 & 0.001 & 0 & 0 \\ 0 & 0 & 0 & 0.001 & 0 \\ 0 & 0 & 0 & 0 & 0.001 \end{bmatrix}$
α	1
Optimization time	$t \leq 30s$
Solver	Knitro [55]
State constraints	[0, 1]
Inputs constraints	[0, 1]

The functioning parameters (sizes, operating powers, conversion factors and costs) of the greenhouse energy systems are depicted in Table 3:

The meteorological data from 2019 are considered for the simulation, and they were extracted from the database Modern-Era Retrospective analysis for Research and Applications version 2 (MERRA-2) [56]. The variables considered are outside temperature, sky temperature, sun radiation, wind speed and relative humidity. In addition, the outside CO_2 level is considered constant during all simulations with 400 ppm.

Table 2: Agricultural greenhouse system parameters.

Parameters	Symbols	Values per hectare	
Area	A_{gh}	60 000 m^2	6 ha
Greenhouse height	h_{gh}	4 m	-
Crops	-	Tomatoes	-
Lighting power	E_{gh}	1.8 MW	0.3 MW ha^{-1}
Boiler power	H_{bl}	6.6 MW	1.1 MW ha^{-1}
CHP heat power	H_{chp}	4.4 MW	0.73 MW ha^{-1}
CHP electricity power	E_{chp}	4.4 MW	0.73 MW ha^{-1}
TES volume	V_{tes}	1500 m^3	250 m^3 ha^{-1}
TES temperatures:			
$SOC = 1$	-	90 °C	-
$SOC = 0$	-	55 °C	-

Energy demand predictions of greenhouse consumption are mandatory for the proposed controller in this work, more specifically for the third and second levels (steady state and dynamic optimization). In this study, the predictions are considered perfect, and they were taken from a dataset generated from a previous simulation with the 2019 meteorological data. Then the energy demands of the agricultural greenhouse were recorded (heat, electricity and CO_2). During the simulation only the boiler was controlled with a rule-based controller with the purpose of maintaining the heat storage from $SOC = 0$ to $SOC = 1$.

The low level (first level) controller set points are tuned as follows:

- Greenhouse temperature: The set points of the PID that control the pumps of the heating networks are: 22 °C between 6 a.m. and 9 p.m. and 20 °C the rest of the day.

- Greenhouse humidity: the windows are open when the humidity relative to concentration exceeds 85 %;

Table 3: Steady state optimization constraints and costs parameters.

Parameters	Boiler	CHP	Storage	Grids
Stopping power	0 MW	0 MW	-	
Minimum operating power	0.5 MW	2.2 MW	-	
Maximum operating power	6.5 MW	4.4 MW	-	
Minimum operating time	1 h	5 h	-	
Minimum downtime	1 h	10 h	-	
Maximum load power	-	-	9.9 MWh	
$C_{\bullet,G\_to\_H}$	0.92	0.35	-	-
$C_{\bullet,G\_to\_CO_2}$	5.7×10^{-8}	-	-	1
$C_{\bullet,G\_to\_E}$	-	0.35	-	1
Discharging maximal power	-	-	$+\infty$	
Minimum storage	-	-	102 MWh	
Maximum storage	-	-	150.8 MWh	
Minimal terminal constraint	-	-	121 MWh	
Maximal terminal constraint	-	-	131 MWh	
Start-up cost	-	200 €		
Natural gas cost	-	-	-	20 € MWh^{-1}
CO_2 cost	-	-	-	150 € t^{-1}
Electrical cost	-	-	-	Day ahead price of 2019

- Greenhouse CO_2: The set point CO_2 concentration is 1000 ppm between 6 a.m. and 9 p.m.. During the rest of the day, there is no set point concentration.
- Plant radiation: The lamps are allowed to operate between 6 a.m. and 9 p.m. and are controlled by a hysteresis from sun radiation with a high threshold of 120 W m^{-2} and a low threshold of 40 W m^{-2}.
- Tomatoes' thermal comfort (thermal and sun screen): The set point for closing

or opening the thermal screen is set with a sun radiation threshold of $35\,\mathrm{W\,m^{-2}}$. The sun screen is controlled according to temperature and sun radiation by two hysteresis connected to an AND gate. The temperature hysteresis has a low threshold of 27 °C and a high threshold of 30 °C. The sun radiation hysteresis has a low threshold of $900\,\mathrm{W\,m^{-2}}$ and a high threshold of $1000\,\mathrm{W\,m^{-2}}$. Finally, to protect the tomatoes, windows are open if the temperature in the greenhouse exceeds the set point temperature by 2 °C.

6. Results and discussion

The results are separated into two distinct sections. Section 6.1 discusses the results of system identification, and sub-section 6.2 presents the findings of the MES operation over a year of crop production.

6.1. Neural Network model identification

Table 4 shows the hyper-parameters ranges considered in this work, which were optimized during training using the BlackBoxOptim package [57], according to the methodology proposed in [44]. The hyperparameters selected by the meta-heuristic algorithm can be seen in Table 4. The fidelity measure is equal to 1.01×10^{-7} with the training data and 9.86×10^{-7} with the test data. As a result, this network is chosen for the MPC tuning predictor.

6.2. Analysis of an operating year

The results of the simulations for the conventional controller and for the advanced controller are presented with duration curves. Other subfigures present exogenous variables (radiation, outside temperature) or system variables (greenhouse temperature, heat storage status, CO_2 injection rate, co-generation unit control, boiler control) with iso-contour probability density of the data values in ordinates. These subfigures are synchronized on the x-axis within the duration curves. Therefore, the subfigures always have duration on the abscissa. Cold colors (blue) indicate a low probability of occurrence, and warm colors (red) indicate a high probability of occurrence of the values.

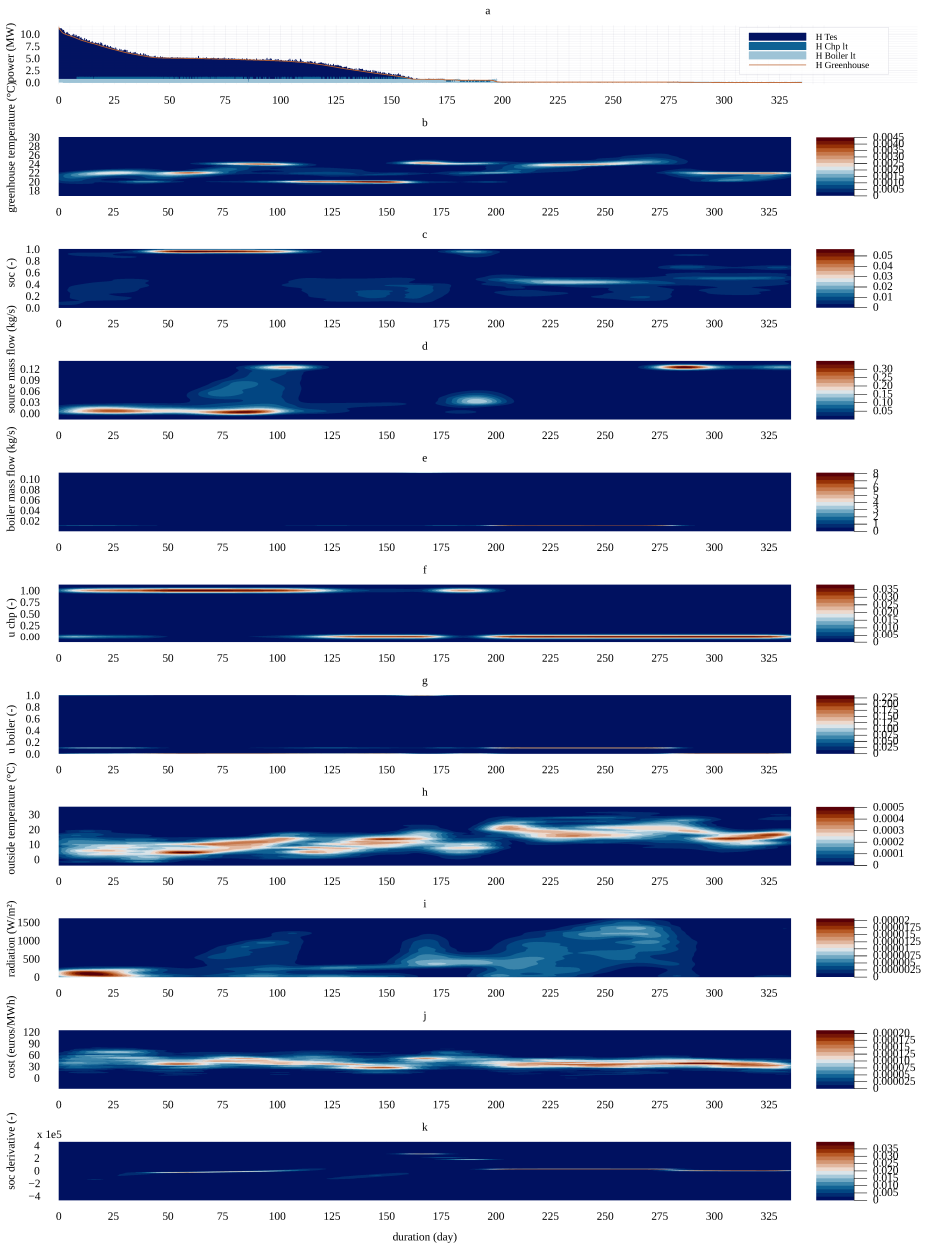

Figure 8: Process control results with the base-line controller : a) greenhouse heat load duration curve. b) greenhouse temperature. c) TES SOC. d) CO_2 flow rate from the source. e) CO_2 flow rate from the boiler. f) input command of the CHP. g) input command of the boiler. h) outside temperature. i) sun radiation.

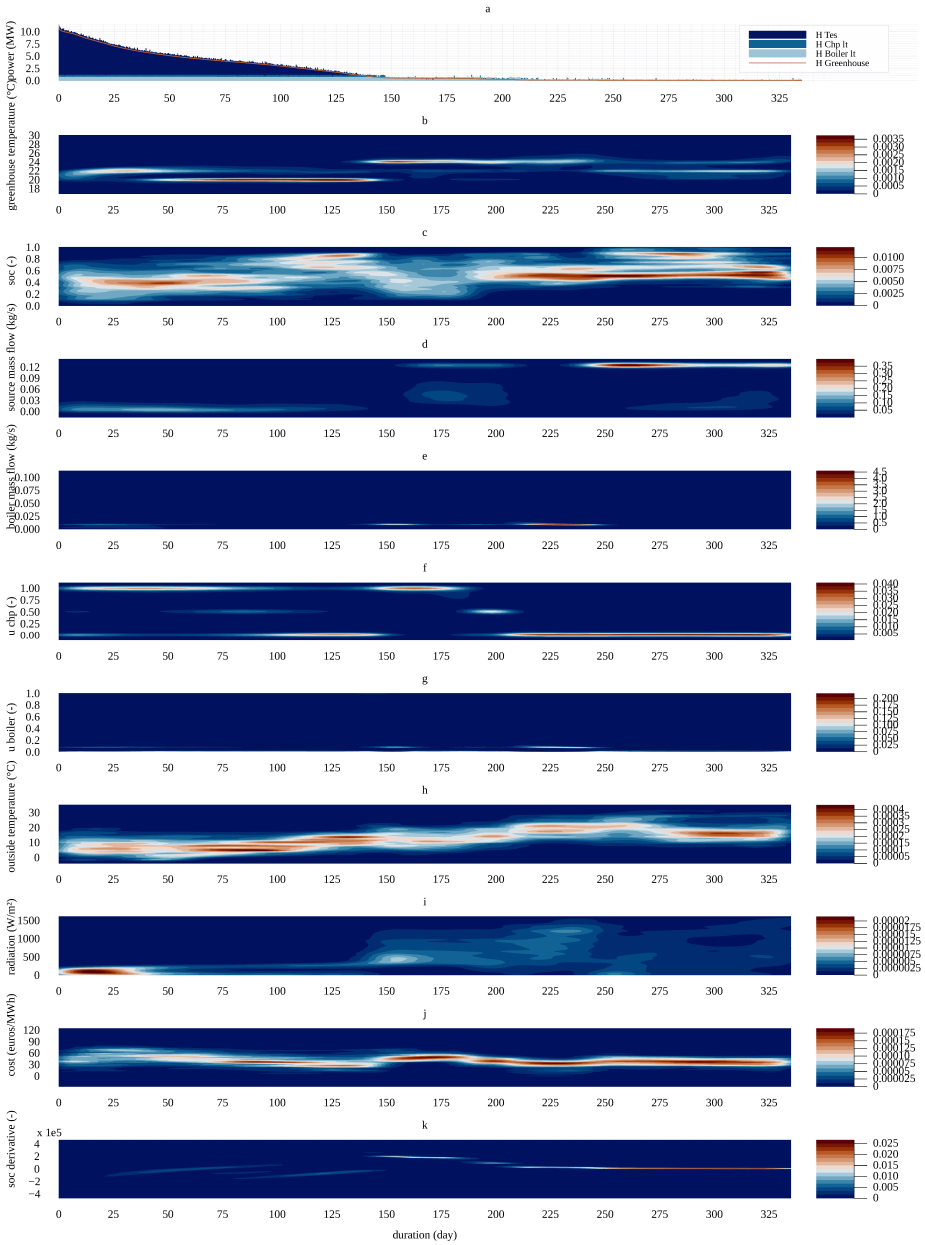

Figure 9: Process control results with the proposed controller. : a) greenhouse heat load duration curve. b) greenhouse temperature. c) TES SOC. d) CO_2 flow rate from the source. e) CO_2 flow rate from the boiler. f) input command of the CHP. g) input command of the boiler. h) outside temperature. i) sun radiation.

Table 4: Hyperparameters range and optimized values.

Parameters	Range Values	Optimized value
Activation function	Relu [58]	Relu
Neurons	5 to 15	8
Hidden layer	1 to 3	3
ResNet layer	1	1
Epoch number	100 to 500	200
Batch size	1024	1024
Optimizer	Adam [59], Radam [60], Nadam [61], Oadam [62][1]	Radam
Learning rate	1×10^{-7} to 0.001	9.71×10^{-4}
Momentum exponential decay	0.9 to 0.999	0.94
Momentum estimate	0.9 to 0.999	0.98

[a] Please note that Radam, Nadam and Oadam are all derived from Adam optimizer.

The punctual comparisons of the figures between the two controllers are limited by the fact that we do not consider the same instants, because the temporal arrangements of the duration curves can differ significantly, but the tendencies and patterns comparison remain informative.

This representation mode highlights recurrent behaviors of the system in a probabilistic way and explains these behaviors by the tendencies of the exogenous data. For example, we can observe the same pattern at the start of both duration curves: the heating load decreases from 11.3 MW at maximum to 5.1 MW at index equivalent on day 35. Thus, these indexes correspond to moments of intense heating of the greenhouse.

For the same indexes and in both cases, iso-contours of occurrences of the internal temperature of the greenhouse show the significant recurrence of values between 20 °C and 22 °C (Figs.8.b 9.b). The iso-contours illustrate occurrences of solar radiation below 250 W m^{-2} (Figs.8.i 9.i) and, most often, low greenhouse outdoor temperatures, less than 10 °C (Figs.8.h 9.h). We can deduce from these observations that the indexes

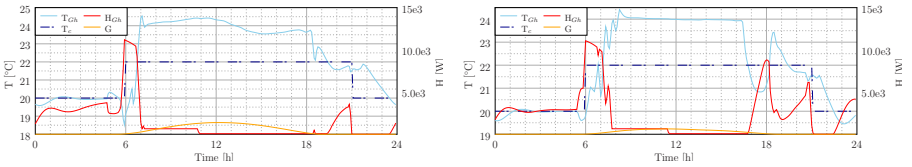

(a) 11 April (b) 03 April

Figure 10: Times series of temperatures in the greenhouse T_{gh} against the set point temperatures T_c (left y-axis) and of the heat provided to the greenhouse H_{gh} against the solar radiation G

correspond to times at the beginning of the day, when the greenhouse temperature set point increases from 20 °C to 22 °C and causes a substantial and instantaneous heat demand.

In addition, for in the rule-based case, we can observe that for the very first indexes, the CHP is frequently set at 0%. This means that, nonintuitively, the indexes of higher heating demands are not solely in winter but between March and November, which can be explained by the use or nonuse of the thermal screen during mid-season days.

Examples of times series of days that includes two of the higher heating loads are shown in Fig.10. We can firstly note that these times series take place in April, and not in the heart of winter as we would intuitively expect. In both cases, we can observe the load peaks take place at 6 a.m. when the set point temperature changes, from 20 °C to 22 °C. The peaks last few tenth of minutes, until the temperature of the greenhouse exceeds the set point, when the sun sets. These time series illustrate and confirm the general observation above.

We can further note that the load duration curves pattern differs from one controller to another, specifically for temporal indexes from the equivalent day 35 to equivalent day 100. A plateau around 4.8 MW (between 5.1 MW and 4.4 MW) can be seen on the load duration curve of the rule-based controller that does not exist for the hierarchical one, which decreases monotonically.

In the rule-based controller case, the co-generation unit operates at its nominal load, and the boiler provides heat while the state of charge of the thermal storage is close to 1. For indexes of equivalent days 37.5 to 75, the highest present occurrences of solar

radiation are above $0\,\mathrm{W\,m^{-2}}$ and achieve $300\,\mathrm{W\,m^{-2}}$ (Fig.8.i), showing that the indexes correspond to specific moments during the day. At these times, the temperature in the greenhouse is frequently 22 °C, respecting the set point. The ambient temperature, usually lower than 10 °C, induces high heat losses that must be compensated for by the heat from the TES since the solar radiations is low. These moments represent the most favorable cases, when there is a balance between the heat produced and supplied to the storage and the heat supplied by the storage to the greenhouse to respect the set point temperature. In the least favorable scenarios, more heat is produced by the co-generation unit and the boiler than what is needed to maintain the set point temperature of the greenhouse and is supplied by the TES. In these cases, the excess heat is dissipated in the greenhouse, the storage having been already saturated. As a consequence, the set point temperature is no longer respected. We can observe this phenomenon for indexes between equivalent days 75 and 100. For these times, the temperature in the greenhouse is often about $24°C$, $2°C$ higher than the set point. The outdoor temperatures are higher than they were previously, between 8 °C and 20 °C (Fig.8.h), and the solar radiation can achieve $1100\,\mathrm{W\,m^{-2}}$ (Fig.8.i). In these conditions, the heat load is low, whereas the production remains high, leading to the greenhouse overheating. An indirect consequence is that the windows of the greenhouse are open causing CO_2 losses that must be compensated for by the CO_2 from the source, explaining the fact that the CO_2 flow rates increase to $0.12\,\mathrm{kg\,s^{-1}}$ (Fig.8.i).

In all cases, the role of the storage is limited because the energy only passes through it. In this respect, the energy system does not seem to be optimized.

Concerning the hierarchical controller, the heat load decreases almost linearly for the same indexes (Fig.9.a). The greenhouse temperatures are mostly maintained at 20 °C but also frequently 22 °C (Fig.9.b.), which are the respective set point temperatures at night and in the day. At the same times, the solar radiation also exhibits two tendencies: either it is around $0\,\mathrm{W\,m^{-2}}$ (nights), or it is above $0\,\mathrm{W\,m^{-2}}$, and it increases nearly linearly as the indexes of the duration curve increase (Fig.9.i) while, the outdoor temperature also increases linearly (Fig.9.h). From these observations, we can deduce that these indexes correspond to moments when the greenhouse follows the set point temperatures in a steady state regime, out of transitions. In these cases, the heat is sup-

plied only to compensate for the losses when solar radiation gains are not enough. The heat supplied here evolves with environmental conditions: when the losses decrease (as the outdoor temperature increases) and the solar gains increase, the load decreases.

Moreover, the SOC varies mostly between 0.2 and 0.6 (Fig.9.h), showing that the TES is duly solicited: it is discharged to provide heat to the greenhouse, and it is charged back without ever having been saturated. It can be seen that the boiler does not operate while the CHP charges the TES, following the load duration curve tendency as it operates successively at its nominal load, then at half load, and finally it is off when the heat load decreases. It is, logically, less solicited when the heating load drops. We can thus conclude that there is an order of priority between the co-generation unit and the boiler, established by the fact that the electricity selling tariff is favorable, most frequently above $30 €\,\mathrm{MW}^{-1}$ (Fig.9.j) against a cost of $20 €\,\mathrm{MW}^{-1}$ for the gas. As an indirect consequence, the CO_2 contribution to the greenhouse is provided by the source (Fig.9.d).

It can be said that the operation of the systems is not energetically optimized with the rule-based controller: the co-generation unit operates by default, the boiler is requested to produce CO_2, and, consequently, the SOC of the storage is usually saturated while the temperatures in the greenhouse regularly exceed the set points. In the case of the hierarchical controller, the systems are energetically optimized: they are used when necessary to recharge the storage, and the SOC varies between 0.4 and 0.6, while the set temperatures are respected, showing that the heat flows in the storage is well regulated. The CHP is preferred to the boiler due to the selling tariff of electricity, and then the source is solicited to supply CO_2 to the greenhouse.

The energy and economic statements for the two controllers are introduced in Table 5. We can observe that the hierarchical controller allows a global heat consumption saving of 28 %, leading to notable economic savings. This energy saving particularly impacts the use of the boiler, which generates only two-thirds of the heat generated in the rule-based controller case, whereas the CHP is used at approximatively the same level for both controllers. Consequently, the hierarchical controller resorts twice more to the CO_2 grid so that the fertilizer cost is multiplied by two. In addition, the electricity generated is comparable with both controllers. However, the incomes from selling

Table 5: Energy and economic statement

	Energy [MWh]		Cost (+) and incomes (-) [€]	
	Base-line	Hierarchical	Base-line	Hierarchical
Greenhouse heat consumption	312	270		
Boiler heat generated	99.55	62.23		
CHP heat generated	212.88	208.07		
CHP electricity generated	212.88	208.07		
Electrical energy exported	187.97	181.24	-8681.1	-9079.6
Electrical energy imported	17.80	15.88	761.6	626.7
	Gas consumption [t]		Cost (+) and incomes (-) [€]	
Natural gas consumption	80.79	76.03	1615.7	1520.6
Total CO_2 consumption	27.22	24.12		
CO_2 consumption (grid)	4.97	10.21	745.5	1531.9
CO_2 consumption (boiler)	22.25	13.91		
Economic statement			-5558.3	-5400.3

electricity are 400 € higher with the hierarchical controller, whereby the CHP produces excess electricity when it is more profitable to be sold. This is not always the case with the rule-based controller. Conversely, the cost of electricity imported from the grid is lower with the hierarchical controller, showing that electricity is bought when the tariffs are the most attractive.

7. Conclusion

A three-level hierarchical control law has been considered in this paper, applied to the multi-energy systems of an agricultural greenhouse. Our work focused more particularly on the second level controller, which must control the dynamics of the multi-energy (ME) systems. The design methodology proposed for level two is based on what we have called ME-MPC. It takes advantage of a dynamic model based on a neural network and captures the nonlinear behavior of energy systems and the greenhouse atmosphere.

The characteristics of a greenhouse in the Pays de la Loire region in France were used for the proof of concept. It produces above-ground tomatoes using different energy flows: electricity, heat and natural gas. CO_2 fertilization was also considered as a flow (input) to be treated. A fine-scale Modelica model of the greenhouse and energy systems led to a very realistic simulator, even taking into account practical solutions to regulate the greenhouse atmosphere, such as thermal and solar screens, artificial lighting, etc. This simulator provides access to all the variables of interest (state of the fine model), allowing a detailed energy analysis. A typical rules-based approach has also been implemented in the simulator to replicate the way greenhouses are currently controlled. This constitutes a reference solution, which made possible a comparative evaluation of the proposed solution. The results obtained constitute a proof of concept of the hierarchical control proposal as a whole. In particular, they validate the ME-MPC level 2 solution as the means of significantly increased energy and economic efficiency.

In summary, the methodology presented in this article offers the following advantages:

- It is a systematic approach that ultimately provides a solution to complex problems by employing hierarchical decomposition of the optimization problem and utilizing a computationally efficient model based on neural networks.
- The level 2 control is applicable to multi-energy systems encountered in the general context of agricultural greenhouses
- Its implementation is likely to reduce engineering time on one hand, and on the other hand, improve the energy performance of agricultural greenhouses by consuming less primary energy and reducing CO_2 emissions.

Some disadvantages have also been highlighted:

- It relies on model-based solutions for data generation, which requires the availability of specific libraries in Modelica that integrate greenhouse or component models. This dependence on specialized libraries can be a limitation.
- The process of calibration or continuous adaptation of the model requires adequate instrumentation of the greenhouses. Sufficient monitoring and measuring devices must be in place for accurate calibration, which may involve additional cost and effort.

Our future work will partly consist of consolidating the management of the CO_2 flow to further reduce the economic balance sheet. The interest (or not) of adding a level of dynamic optimization based on the entire greenhouse model (multi-energy system and climatic atmosphere) could be studied. Finally, applying the approach to an agricultural greenhouse and not to its digital twin is the logical next step.

Acknowledgments

The authors thank the Julia community for online comments about the Julia programming language. This research was funded by Conseil Régional des Pays de la Loire, France. The authors have no financial or proprietary interests in any material discussed in this article.

References

[1] A. J. Hati, R. R. Singh, Smart indoor farms: Leveraging technological advancements to power a sustainable agricultural revolution, AgriEngineering 3 (4) (2021) 728–767. doi:10.3390/agriengineering3040047.

[2] F. Golzar, N. Heeren, S. Hellweg, R. Roshandel, A novel integrated framework to evaluate greenhouse energy demand and crop yield production, Renewable and Sustainable Energy Reviews 96 (2018) 487–501. doi:10.1016/j.rser.2018.06.046.

[3] Y. Su, Q. Yu, L. Zeng, Parameter self-tuning pid control for greenhouse climate control problem, IEEE Access 8 (2020) 186157–186171. doi:10.1109/ACCESS.2020.3030416.

[4] L. Chen, S. Du, D. Xu, Y. He, M. Liang, Sliding mode control based on disturbance observer for greenhouse climate systems, Mathematical Problems in Engineering 2018 (2018) 2071585. doi:10.1155/2018/2071585.

[5] F. Lafont, J.-F. Balmat, Optimized fuzzy control of a greenhouse, Fuzzy Sets and Systems 128 (1) (2002) 47–59. doi:10.1016/S0165-0114(01)00182-8.

[6] M. Nachidi, F. Rodríguez, F. Tadeo, J. Guzman, Takagi–sugeno control of nocturnal temperature in greenhouses using air heating, ISA Transactions 50 (2) (2011) 315–320. doi:10.1016/j.isatra.2010.11.007.

[7] P. van Beveren, J. Bontsema, G. van Straten, E. van Henten, Optimal control of greenhouse climate using minimal energy and grower defined bounds, Applied Energy 159 (2015) 509–519. doi:10.1016/j.apenergy.2015.09.012.

[8] P. Van Beveren, J. Bontsema, G. Van Straten, E. Van Henten, Minimal heating and cooling in a modern rose greenhouse, Applied Energy 137 (2015) 97–109. doi:10.1016/j.apenergy.2014.09.083.

[9] I. Ioslovich, P.-O. Gutman, R. Linker, Hamilton–jacobi–bellman formalism for optimal climate control of greenhouse crop, Automatica 45 (5) (2009) 1227–1231. doi:10.1016/j.automatica.2008.12.024.

[10] A. Ramírez-Arias, F. Rodríguez, J. Guzmán, M. Berenguel, Multiobjective hierarchical control architecture for greenhouse crop growth, Automatica 48 (3) (2012) 490–498. doi:10.1016/j.automatica.2012.01.002.

[11] L. Wang, X. Li, M. Xu, Z. Guo, B. Wang, Study on optimization model control method of light and temperature coordination of greenhouse crops with benefit priority, Computers and Electronics in Agriculture 210 (2023) 107892. doi:https://doi.org/10.1016/j.compag.2023.107892.
URL https://www.sciencedirect.com/science/article/pii/S0168169923002806

[12] D. Q. Mayne, Model predictive control: Recent developments and future promise, Automatica 50 (12) (2014) 2967–2986. doi:10.1016/j.automatica.2014.10.128.

[13] M. L. Darby, M. Nikolaou, Mpc: Current practice and challenges, Control Engineering Practice 20 (4) (2012) 328–342. doi:10.1016/j.conengprac.2011.12.004.

[14] C. Bersani, A. Ouammi, R. Sacile, E. Zero, Model predictive control of smart greenhouses as the path towards near zero energy consumption, Energies 13 (14) (2020). doi:10.3390/en13143647.

[15] W.-H. Chen, N. S. Mattson, F. You, Intelligent control and energy optimization in controlled environment agriculture via nonlinear model predictive control of semi-closed greenhouse, Applied Energy 320 (2022) 119334. doi:https://doi.org/10.1016/j.apenergy.2022.119334.
URL https://www.sciencedirect.com/science/article/pii/S0306261922006845

[16] D. Lin, L. Zhang, X. Xia, Model predictive control of a venlo-type greenhouse system considering electrical energy, water and carbon dioxide consumption, Applied Energy 298 (2021) 117163. doi:https://doi.org/10.1016/j.apenergy.2021.117163.

URL https://www.sciencedirect.com/science/article/pii/S0306261921005973

[17] S. Piñón, E. Camacho, B. Kuchen, M. Peña, Constrained predictive control of a greenhouse, Computers and Electronics in Agriculture 49 (3) (2005) 317–329, modelling and control in agricultural processes. doi:10.1016/j.compag.2005.08.007.

[18] M. El Ghoumari, H.-J. Tantau, J. Serrano, Non-linear constrained mpc: Real-time implementation of greenhouse air temperature control, Computers and Electronics in Agriculture 49 (3) (2005) 345–356, modelling and control in agricultural processes. doi:10.1016/j.compag.2005.08.005.

[19] L. Chen, S. Du, Y. He, M. Liang, D. Xu, Robust model predictive control for greenhouse temperature based on particle swarm optimization, Information Processing in Agriculture 5 (3) (2018) 329–338. doi:10.1016/j.inpa.2018.04.003.

[20] M. C. Bozchalui, C. A. Cañizares, K. Bhattacharya, Optimal energy management of greenhouses in smart grids, IEEE Transactions on Smart Grid 6 (2) (2015) 827–835. doi:10.1109/TSG.2014.2372812.

[21] D.-H. Jung, H. S. Kim, C. Jhin, H.-J. Kim, S. H. Park, Time-serial analysis of deep neural network models for prediction of climatic conditions inside a greenhouse, Computers and Electronics in Agriculture 173 (2020) 105402. doi:https://doi.org/10.1016/j.compag.2020.105402.

[22] T. Moon, S. Hong, H. Y. Choi, D. H. Jung, S. H. Chang, J. E. Son, Interpolation of greenhouse environment data using multilayer perceptron, Computers and Electronics in Agriculture 166 (2019) 105023. doi:https://doi.org/10.1016/j.compag.2019.105023.

[23] F. Mahmood, R. Govindan, A. Bermak, D. Yang, T. Al-Ansari, Data-driven robust model predictive control for greenhouse temperature control and energy utilisation assessment, Applied Energy 343 (2023) 121190.

doi:https://doi.org/10.1016/j.apenergy.2023.121190.
URL https://www.sciencedirect.com/science/article/pii/S0306261923005548

[24] K. López-Aguilar, A. Benavides-Mendoza, S. González-Morales, A. Juárez-Maldonado, P. Chiñas-Sánchez, A. Morelos-Moreno, Artificial neural network modeling of greenhouse tomato yield and aerial dry matter, Agriculture 10 (4) (2020). doi:10.3390/agriculture10040097.

[25] D.-H. Jung, H.-J. Kim, J. Y. Kim, T. S. Lee, S. H. Park, Model predictive control via output feedback neural network for improved multi-window greenhouse ventilation control, Sensors 20 (6) (2020). doi:10.3390/s20061756.

[26] A. Ouammi, Y. Achour, H. Dagdougui, D. Zejli, Optimal operation scheduling for a smart greenhouse integrated microgrid, Energy for Sustainable Development 58 (2020) 129–137. doi:10.1016/j.esd.2020.08.001.

[27] A. Ouammi, Y. Achour, D. Zejli, H. Dagdougui, Supervisory model predictive control for optimal energy management of networked smart greenhouses integrated microgrid, IEEE Transactions on Automation Science and Engineering 17 (1) (2020) 117–128. doi:10.1109/TASE.2019.2910756.

[28] Y. Achour, A. Ouammi, D. Zejli, S. Sayadi, Supervisory model predictive control for optimal operation of a greenhouse indoor environment coping with food-energy-water nexus, IEEE Access 8 (2020) 211562–211575. doi:10.1109/ACCESS.2020.3037222.

[29] P. van Beveren, J. Bontsema, G. van Straten, E. van Henten, Optimal utilization of a boiler, combined heat and power installation, and heat buffers in horticultural greenhouses, Computers and Electronics in Agriculture 162 (2019) 1035–1048. doi:10.1016/j.compag.2019.05.040.

[30] P. van Beveren, J. Bontsema, A. van 't Ooster, G. van Straten, E. van Henten, Optimal utilization of energy equipment in a semi-closed greenhouse, Computers

and Electronics in Agriculture 179 (2020) 105800. doi:10.1016/j.compag.2020.105800.

[31] N. Van den Bulck, M. Coomans, L. Wittemans, J. Hanssens, K. Steppe, Monitoring and energetic performance analysis of an innovative ventilation concept in a belgian greenhouse, Energy and Buildings 57 (2013) 51–57. doi:10.1016/j.enbuild.2012.11.021.

[32] C. Tsay, M. Baldea, 110th anniversary: using data to bridge the time and length scales of process systems, Industrial & Engineering Chemistry Research 58 (36) (2019) 16696–16708. doi:10.1021/acs.iecr.9b02282.

[33] A. Parisio, C. Del Vecchio, A. Vaccaro, A robust optimization approach to energy hub management, International Journal of Electrical Power & Energy Systems 42 (1) (2012) 98–104. doi:10.1016/j.ijepes.2012.03.015.

[34] K. R. Muske, J. B. Rawlings, Model predictive control with linear models, AIChE Journal 39 (2) (1993) 262–287. doi:10.1002/aic.690390208.

[35] L. Grüne, J. Pannek, Nonlinear Model Predictive Control, Springer International Publishing, Cham, 2017, pp. 43–66. doi:10.1007/978-3-319-46024-6_3.

[36] L. A. de Araujo Passos, T. J. Ceha, S. Baldi, B. De Schutter, Model predictive control of a thermal chimney and dynamic solar shades for an all-glass facades building, Energy 264 (2023) 126177. doi:https://doi.org/10.1016/j.energy.2022.126177.
URL https://www.sciencedirect.com/science/article/pii/S0360544222030638

[37] P. C. Blaud, P. Chevrel, F. Claveau, P. Haurant, A. Mouraud, From multi-physics models to neural network for predictive control synthesis, Optimal Control Applications and Methods n/a (n/a) (2021) 1–18. doi:https://doi.org/10.1002/oca.2845.
URL https://onlinelibrary.wiley.com/doi/abs/10.1002/oca.2845

[38] S. E. Mattsson, H. Elmqvist, M. Otter, Physical system modeling with modelica, Control Engineering Practice 6 (4) (1998) 501–510. doi:10.1016/S0967-0661(98)00047-1.

[39] Q. Altes-Buch, S. Quoilin, V. Lemort, Greenhouses: A modelica library for the simulation of greenhouse climate and energy systems, in: Proceedings of the 13th International Modelica Conference, Vol. 157, 2019, pp. 533–542. doi:10.3384/ecp19157533.

[40] L. Andresen, P. Dubucq, R. P. Garcia, G. Ackermann, A. Kather, G. Schmitz, Status of the transient library: Transient simulation of coupled energy networks with high share of renewable energy, in: Proceedings of the 11th International Modelica Conference, Vol. 118, 2015, pp. 695–705. doi:10.3384/ecp15118695.

[41] B. Recht, Reflections on the learning-to-control renaissance, in: Proceedings of the 21st IFAC World Congress, 2020.
URL https://www.youtube.com/watch?v=IEZFwh8sw8s

[42] J. B. Rawlings, C. T. Maravelias, Bringing new technologies and approaches to the operation and control of chemical process systems, AIChE Journal 65 (6) (2019) e16615. arXiv:https://aiche.onlinelibrary.wiley.com/doi/pdf/10.1002/aic.16615, doi:https://doi.org/10.1002/aic.16615.

[43] K. He, X. Zhang, S. Ren, J. Sun, Identity mappings in deep residual networks, in: B. Leibe, J. Matas, N. Sebe, M. Welling (Eds.), Computer Vision – ECCV 2016, Springer International Publishing, Cham, 2016, pp. 630–645.

[44] P. C. Blaud, P. Chevrel, F. Claveau, P. Haurant, A. Mouraud, Resnet and polynet based identification and (mpc) control of dynamical systems: a promising way, IEEE Access (2022) 1–1doi:10.1109/ACCESS.2022.3196920.

[45] P. Blaud, Pilotage distribué de systèmes multi-énergies en réseau, Ph.D. thesis, IMT Atlantique, ch. 2-3 (2022).
URL https://theses.hal.science/tel-03681888/

[46] S. de Oliveira Kothare, M. Morari, Contractive model predictive control for constrained nonlinear systems, IEEE Transactions on Automatic Control 45 (6) (2000) 1053–1071. doi:10.1109/9.863592.

[47] K. Åström, T. Hägglund, The future of pid control, Control Engineering Practice 9 (11) (2001) 1163–1175. doi:10.1016/S0967-0661(01)00062-4.

[48] S. D. Cohen, A. C. Hindmarsh, P. F. Dubois, Cvode, a stiff/nonstiff ode solver in c, Computers in physics 10 (2) (1996) 138–143.

[49] I. Dunning, J. Huchette, M. Lubin, Jump: A modeling language for mathematical optimization, SIAM review 59 (2) (2017) 295–320. doi:10.1137/15M1020575.

[50] J. Bezanson, A. Edelman, S. Karpinski, V. B. Shah, Julia: A fresh approach to numerical computing, SIAM review 59 (1) (2017) 65–98. doi:10.1137/141000671.

[51] R. Lougee-Heimer, The common optimization interface for operations research: Promoting open-source software in the operations research community, IBM Journal of Research and Development 47 (1) (2003) 57–66. doi:10.1147/rd.471.0057.

[52] M. Innes, Flux: Elegant machine learning with julia, Journal of Open Source Software 3 (25) (2018) 602. doi:10.21105/joss.00602.

[53] K. Gao, G. Mei, F. Piccialli, S. Cuomo, J. Tu, Z. Huo, Julia language in machine learning: Algorithms, applications, and open issues, Computer Science Review 37 (2020) 100254. doi:10.1016/j.cosrev.2020.100254.

[54] J. Revels, M. Lubin, T. Papamarkou, Forward-mode automatic differentiation in julia, CoRR abs/1607.07892 (2016). arXiv:1607.07892.
URL http://arxiv.org/abs/1607.07892

[55] R. H. Byrd, J. Nocedal, R. A. Waltz, Knitro: An integrated package for nonlinear optimization, Springer US, Boston, MA, 2006, pp. 35–59. doi:10.1007/0-387-30065-1_4.

[56] Global modeling and assimilation office (gmao), merra-2 tavg1_2d_slv_nx:2d,1-hourly,time-averaged,single-level,assimilation,single-level diagnostics v5.12.4, Goddard Earth Sciences Data and Information Services Center (GES DISC) (2015). doi:10.5067/VJAFPLI1CSIV,disponible.
URL http://www.soda-pro.com/

[57] R. Feldt, A. Stukalov, Blackboxoptim.jl, GitHub repository (2018).
URL https://github.com/robertfeldt/BlackBoxOptim.jl

[58] D. Smith, H. LeBlanc, Variable activation functions and spawning in neuroevolution, in: Proceedings of the 2018 ASEE North Central Section Conference, 2018.

[59] D. P. Kingma, J. Ba, Adam: A method for stochastic optimization, in: International Conference on Learning Representations (ICLR), 2015.

[60] L. Liu, H. Jiang, P. He, W. Chen, X. Liu, J. Gao, J. Han, D. P. Kingma, J. Ba, On the variance of the adaptive learning rate and beyond, in: International Conference on Learning Representations (ICLR), 2020.

[61] T. Dozat, Incorporating nesterov momentum into adam, in: International Conference on Learning Representations (ICLR), 2016.

[62] C. Daskalakis, A. Ilyas, V. Syrgkanis, H. Zeng, Training gans with optimism, in: International Conference on Learning Representations (ICLR), 2018.